Proceedings of the 2006 IEEE International Conference on Robotics and Automation
Orlando, Florida - May 2006

Study on the 3D Shape of Active Cord Mechanism

Hiroya Yamada, Shigeo Hirose
Department of Mechanical and Aerospace Engineering
Tokyo Institute of Technology
2-12-1 O-okayama Meguro-ku Tokyo 152-8522 Japan
Email: yamada@robotics.mes.titech.ac.jp

***Abstract*— Snake-like robots and hyper-redundant manipulators have been called *Active Cord Mechanism* (ACM), and they have been one of fields of robotics. However, general study on the spatial shape of ACM has not been conducted enough so far. In this paper, we propose a effective method for analysis of the 3D shape of ideal continuous ACM models. In addition, we show some important characteristics of ACM using this method. The results help us understand the characteristics and possibility of ACM.**

I. Introduction

Snake-like robots and hyper-redundant manipulators have been studied as one of fields of robotics. They are classified into “Active Cord Mechanism (ACM) ”, which is defined as “functional body which connects in a series joint units, and which forms a cord” [1]. The concept of ACM includes not only robots but also organisms such as snakes, legs of octopuses, trunks of elephants and so on. Though ACM has simple structure composed of series of joints, it has the ability to conduct various functions by changing the shape cleverly. That is why researchers have studied on ACM. Since the study have started from the first snake-like robot which realized the creeping motion of snakes on a plain[1], various snake-like robots and hyper-redundant manipulators have been developed. Today some of mechanical ACM models are able to move spatially as shown in Fig. 1, which shows our new 3-dimensional snake-like robot.

Generally speaking, mechanical ACM models have their unique structures, so the characteristics such as the number of joints and the dimension of the body are special to each model. So when we discuss about the shape control of ACM, we need to consider the structure of each model. However, as we mentioned above, ACM means “functional body which forms a cord” , so we can expect that all ACM have some common features due to the form of cord. When we study such common features of ACM, we can forget the details of mechanical ACM models and introduce an ideal model of ACM.

The ideal ACM model has been used effectively in the study of 2-dimensinal ACM. In this case, the ideal ACM model is equal to a plane curve. For example, in the field of snake-like robots, the analysis of creeping motion of snakes have succeeded using a plane curve as the model of a snake[1]. Plane curves have been also used for path planning of snake-like robots and vehicles, and redundant manipulators. Those facts show that the ideal ACM model is useful for both of analysis and application of ACM.

Fig. 1. 3-D Active Cord Mechanism

But the ideal ACM models have not been used sufficiently so far in the study on 3-dimensional ACM. The research in 1990s conducted by Chirikjian et al. is important as an example which using the ideal ACM model[2]. After that research Mochiyama et al. have studied the shape control of redundant manipulator using spatial curves[3], and Date et al. have researched the statics of 3-D snake-like robots with a continuous model[4]. Recently, Jones and Walker et al. have proposed a method to control continuous robots which consist of a serial connenction of finete constant cuvature sections[5]. But, until now the general discussion on the shape of 3-D ACM has not been enough.

So we have worked to introduce a ideal 3-D ACM model and investigate the characteristics of ACM.

In this paper, we discuss the study on the shape of ACM using the ideal ACM model. In section II, we describe what is the ideal ACM model and introduce the prior researches. In section III, we propose differential equations which represent ACM’s shape, and classify ACM into 4 important group. In section IV, we prove ACM’s important characteristics using the ideal model. In section V, conclusion and future work are described.

II. Ideal ACM Model and Prior Research

A. Ideal ACM Model

ACM is defined as “functional body which forms a cord”, so the ideal model of ACM should have a continuous and smooth body like a cord. In order to emphasis the smoothness of ideal model let us call the ideal ACM model as “continuous model”. In this section, we discuss what is a continuous model of ACM.

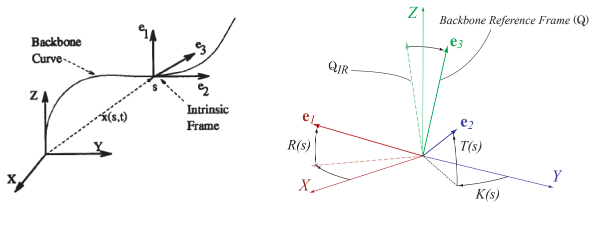

(a) Backbone Curve (b) Backbone Frame

Fig. 2. Chirikjian's model

Intuitively we may think of a spatial curve for continuous model of 3-D ACM. But a spatial curve is not sufficient in fact, because a curve consists of a set of points but continuous ACM model is composed of a set of small elements of rigid body. The state of a point is fixed by its coordinates, but as for rigid body both of coordinates and postures are required to fix its state; Information about the posture is necessary in order to define the shape of continuous ACM model in addition to a spatial curve. Fig. 7 shows a snake winding itself around a branch[6]. It clearly shows the necessity of information about the direction of the back and belly to express the shape of a snake.

B. Prior Research

The discussion in section II-A have been also pointed out in prior research. In the research of Chirikjian et al mentioned in section 1, they proposed the concept of "*backbone curve reference set*". *backbone curve reference set* is composed of "*backbone curve*", which expresses the coordinates of backbone of ACM and "*backbone reference frame*", which is put on the backbone curve and shows the direction of body of ACM as shown in Fig. 2(a). This *backbone curve reference set* is equal to a ideal ACM model. The shape of *backbone curve reference set* is calculated as following. The backbone curve is consisting of small elements of line. Firstly the direction of the elements are fixed with function $K(s)$ and $T(s)$ with respect to a fixed coordinate frame as shown in Fig. 2(b) along the whole body of ACM ($\mathbf{e_2}$ shows the direction of an element). The set of small elements becomes the backbone curve. Where s is the arc-length parameter measuring the distance from the base along the curve, and $K(s)$ and $T(s)$ are the functions of s. When we set the base on the origin of the fixed frame, the coordinates of backbone curve at $s = s_0$ are calculated through following equations; The shape of a backbone curve is determined by $K(s)$ and $T(s)$.

$$\mathbf{x}(s_0) = \begin{pmatrix} \int_0^{s_0} \cos T(s) \sin K(s) ds \\ \int_0^{s_0} \cos T(s) \cos K(s) ds \\ \int_0^{s_0} \sin T(s) ds \end{pmatrix} \tag{1}$$

After the settlement of backbone curve, the posture of backbone reference frame ($\mathbf{Q}$) is fixed with function $R(s)$ and $\mathbf{Q_{IR}}$ as shown in Fig. 2(b). $\mathbf{Q_{IR}}$ is called *induced frame*, and it is determined by $K(s)$ and $T(s)$. After all, a backbone curve reference set is a function of $K(s)$, $T(s)$, and $R(s)$. These 3 functions is called *shape functions*, and Chirikjian et al. have studied analysis and control of ACM using above method.

(a) Bellows with a Line

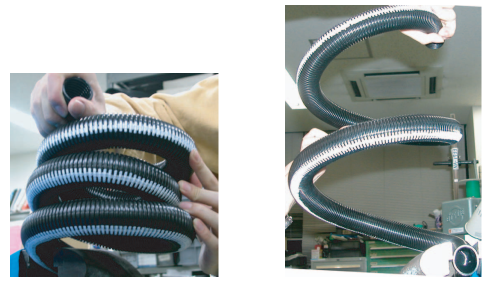

(b) Example (1) (c) Example (2)

Fig. 3. Spiral of Bellows

However, there are some problems which are difficult for this method to deal with. In this method the shape of ACM is determined with respect to a fixed coordinate frame, so local deformation such as "bending" and "torsion" are intuitive. Fig. 3 shows an example of such problems. Firstly, a straight line was drawn on a bellows pipe in straight shape (Fig. 3(a)). Secondly, that bellows was bend to form a spiral (Fig. 3(b), (c)). As shown in Fig. 3(b), (c), the line which was straight at first got twisted. This phenomenon is caused by bellows' characteristics of "able to be bent but not twisted" as shown in section IV, but Chirikjian's method is not suitable to deal with this character. We need the other method for this kind of problem.

We propose a method to express the shape of continuous ACM model in next section, which can deal with torsion and bending directly. Then we clarify some important features of ACM using it.

III. Shape Equations of ACM

A. Shape Equations

As mentioned in section II a spatial curve is not sufficient to express the shape of ACM. But, the theory on spatial curves is available when we produce a model of ACM, so we make brief explanation of it. According to classical differential geometry, the shape of a spatial curve is determined by 2 functions: curvature $\kappa(s)$ and torsion $\tau(s)$. Where s is the arc length which measures the distance from the base along the curve. This means that $\kappa(s)$ and $\tau(s)$ are distributed around the curve. The shape of a curve is calculated through following Frenet-

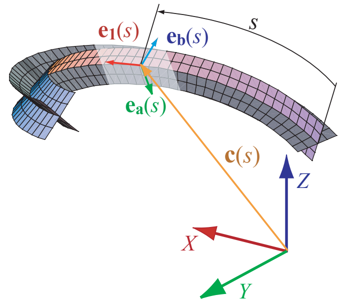

Fig. 4. Dorsal Reference Curve

Serret equations.

$$\left\{\begin{array}{rcl} \dfrac{d\mathbf{c}}{ds} &=& \mathbf{e_1} \\ \dfrac{d\mathbf{e_1}}{ds} &=& \kappa(s)\mathbf{e_2} \\ \dfrac{d\mathbf{e_2}}{ds} &=& -\kappa(s)\mathbf{e_1} + \tau(s)\mathbf{e_3} \\ \dfrac{d\mathbf{e_3}}{ds} &=& -\tau(s)\mathbf{e_2} \end{array}\right. \tag{2}$$

Where $\mathbf{c} = \{x(s), y(s), z(s)\}$ is the coordinates of the curve at s. $\kappa(s)$ and $\tau(s)$ are a curvature and a torsion respectively as mentioned above. $\{\mathbf{e_1}, \mathbf{e_2}, \mathbf{e_3}\}$ is a orthonormal frame; $\mathbf{e_1}$ is defined as a tangential unit vector of the backbone curve, $\mathbf{e_2}$ is defined as an unit vector looking to the direction of bending of the curve, and $\mathbf{e_3}$ is defined as $\mathbf{e_3} = \mathbf{e_1} \times \mathbf{e_2}$. So this frame is fixed by the shape of the curve. The meaning of (2) is explained as follows; A moving frame $\{\mathbf{e_1}, \mathbf{e_2}, \mathbf{e_3}\}$ is going forward in direction of $\mathbf{e_1}$ with rotation represented by an angular velocity vector $(\tau(s)\mathbf{e_1} + \kappa(s)\mathbf{e_3})$ with respect to s, and the locus of the frame makes the curve $\mathbf{c}$. Curvature $\kappa(s)$ is the rate of bending, and torsion $\tau(s)$ is the rate of twist at point s. These 2 functions determine the shape of a curve.

As mentioned in section II-B, a space curve is not enough for ACM. In order to determine the shape of ACM we need 3 functions as known from Chirikjian's research, though as for a spatial curve we need 2 functions. So we introduce following equations, which is an extension of Frenet-Serret equations (2).

$$\left\{\begin{array}{rcl} \dfrac{d\mathbf{c}}{ds} &=& \mathbf{e_1} \\ \dfrac{d\mathbf{e_1}}{ds} &=& \kappa_b(s)\mathbf{e_a} - \kappa_a(s)\mathbf{e_b} \\ \dfrac{d\mathbf{e_a}}{ds} &=& -\kappa_b(s)\mathbf{e_1} + \tau(s)\mathbf{e_b} \\ \dfrac{d\mathbf{e_b}}{ds} &=& \kappa_a\mathbf{e_1} - \tau(s)\mathbf{e_a} \end{array}\right. \tag{3}$$

Let us call (3) as "*ACM's shape equations*" or just "*shape equations*". As a matter of form, (3) is obtained just by adding 2 terms to (2). $\mathbf{c}$ and $\mathbf{e_1}$ represent the coordinates and tangential vector of a curve respectively, and that is the same as (2). But the definitions of $\mathbf{e_a}$, $\mathbf{e_b}$ are different from that of $\mathbf{e_2}$, $\mathbf{e_3}$ in (2). Though $\mathbf{e_2}$, $\mathbf{e_3}$ are defined from the shape of a curve, $\mathbf{e_a}$, $\mathbf{e_b}$ represent the direction of a ACM's body such as the belly or the back. In addition, the angular velocity vector of the frame $\{\mathbf{e_1}, \mathbf{e_a}, \mathbf{e_b}\}$ has 3-axis components as $(\tau(s)\mathbf{e_1} + \kappa_a(s)\mathbf{e_a} + \kappa_b(s)\mathbf{e_b})$. This enables the frame $\{\mathbf{e_1}, \mathbf{e_a}, \mathbf{e_b}\}$ to be separated from the shape of a curve and represent the posture of an ACM's body. (3) can be integrated analytically or numerically with given initial condition and τ, κ_a and κ_b, and a solution $\{\mathbf{c}, \mathbf{e_1}, \mathbf{e_a}, \mathbf{e_b}\}$ is obtained. Now we note that the frame $\{\mathbf{e_1}, \mathbf{e_a}, \mathbf{e_b}\}$ represent the posture of ACM's body but we do not need to fix the direction of $\mathbf{e_a}$ and $\mathbf{e_b}$ here like "$\mathbf{e_a}$ shows the belly and $\mathbf{e_b}$ shows the right side". It is free how to decide the physical direction of $\mathbf{e_a}$ and $\mathbf{e_b}$.

Fig. 4 shows an example of a solution of (3). This figure shows the backbone curve and the locus drawn by $\mathbf{e_a}(s), \mathbf{e_b}(s)$, which are fixed to the backbone curve. Because this figure looks like a slender fish which has a long dorsal fin, let us call a solution of (3) as a "*dorsal reference curve*", and let us call a frame $\{\mathbf{e_1}, \mathbf{e_a}, \mathbf{e_b}\}$ as a "*dorsal reference frame*". Dorsal reference curve consists of a backbone curve and a dorsal reference frame. In addition, we call 3 functions $\tau(s)$, $\kappa_a(s)$ and $\kappa_b(s)$ as shape functions after Chirikjian's research.

(3) is a natural extension of Frenet-Serret equations (2), so in fact some researchers have reached the almost same idea [3][4]. But their research was not enough to deal with general theory on ACM, so we use our expression (3) in our research.

Compared with Chirikjian's method introduced in section II, our method has some advantages because it handles bending and torsion of ACM directly.

B. Classification of ACM

As mentioned above 3 shape functions $\tau(s)$, $\kappa_a(s)$ and $\kappa_b(s)$ determine the shape of ACM. These functions are available to classify ACM into 4 important groups, and this classification is efficient to clarify the characteristics of ACM.

1) Planar Model ($\tau(s) = \kappa_a(s) = 0$): Planar model is defined by the condition of $\tau(s) = 0$ and $\kappa_a(s) = 0$. Planar model is identical with a planar curve, because the shape equations of planar model is equal to equations of a planar curve. The characteristics of a planar curve can be understood intuitively, so we do not need to discuss it here.

2) Frenet-Serret Model ($\kappa_a = 0$): Frenet-Serret model is defined by the condition of $\kappa_a(s) = 0$. The shape equations of Frenet-Serret model is equal to Frenet-Serret equations, so the theory on spatial curves is available to investigate the characteristics as discussed in next section.

3) Bellows Model ($\tau = 0$): Bellows model is defined by the condition of $\tau(s) = 0$. This means it has a feature of *being able to be bend but not to be twisted* like bellows. Most of ACM developed in the world so far belongs to this group, so this is the most important model. The study on this model using continuous model have not been sufficient so far.

4) Complete Model: Complete model is defined as a model which has no restriction about the shape functions. So complete model can realize all dorsal reference curve, which means it can vary the direction of the dorsal reference maintaining the backbone curve.

IV. Characteristics of ACM

In this section we discuss the characteristics of ACM using continuous ACM model.

A. Frenet-Serret Model

According to differential geometry, any spatial curve are uniquely determined by a pair of curvature and torsion, and the opposite is true. This means that Frenet-Serret model can adapt any spatial curve as the backbone curve, but the dorsal reference frame is uniquely fixed by that curve. Because of this characteristics Frenet-Serret model is available as a model of ACM such as hyper-redundant manipulators.

B. Bellows Model

Firstly, we show the fact that bellows model is able to draw any backbone curve at will. This fact is important, because typical snake-like robots are represented by this model. In order to prove this, We investigate the condition which makes both of bellows model and Frenet-Serret model have a same backbone curve. If that condition exists at all times it is proved that bellows model is capable of make all backbone curves, because as shown above section Frenet-Serret model can adapt any backbone curve. The shape equations of Frenet-Serret model is as follows:

$$\left\{\begin{array}{lllll} \frac{d\mathbf{c_F}}{ds} & = & & \mathbf{e_{F1}} & \\ \frac{d\mathbf{e_{F1}}}{ds} & = & & \kappa_{Fb}(s)\mathbf{e_{Fa}} & \\ \frac{d\mathbf{e_{Fa}}}{ds} & = & -\kappa_{Fb}(s)\mathbf{e_{F1}} & & +\tau_F(s)\mathbf{e_{Fb}} \\ \frac{d\mathbf{e_{Fb}}}{ds} & = & & -\tau_F(s)\mathbf{e_{Fa}} & \end{array}\right. \tag{4}$$

(4) is equal to Frenet-Serret equations (2) except for the suffixes. The suffix "F" means Frenet-Serret model. The shape equations of bellows model is as follows:

$$\left\{\begin{array}{lllll} \frac{d\mathbf{c_B}}{ds} & = & & \mathbf{e_{B1}} & \\ \frac{d\mathbf{e_{B1}}}{ds} & = & & \kappa_{Bb}(s)\mathbf{e_{Ba}} & -\kappa_{Ba}(s)\mathbf{e_{Bb}} \\ \frac{d\mathbf{e_{Ba}}}{ds} & = & -\kappa_{Bb}(s)\mathbf{e_{B1}} & & \\ \frac{d\mathbf{e_{Bb}}}{ds} & = & \kappa_{Ba}\mathbf{e_{B1}} & & \end{array}\right. \tag{5}$$

(5) is obtained by substituting $\tau(s) = 0$ in (3). The suffix "B" means bellows model. When 2 models draw a same backbone curve, obviously $\mathbf{c_F} = \mathbf{c_B}$ and $\mathbf{e_{F1}} = \mathbf{e_{B1}}$ hold true. So we investigate the condition when (4), (5), $\mathbf{c_F} = \mathbf{c_B}$ and $\mathbf{e_{F1}} = \mathbf{e_{B1}}$ are true. As a preparation, we introduce a function $\phi(s)$ defined in Fig. 5. $\phi(s)$ helps us operate the equations easily. Now $\phi(s)$ is an unknown function. According to the definition of $\phi(s)$, the following equations are obtained.

$$\mathbf{e_{Ba}} = \cos\phi\mathbf{e_{Fa}} - \sin\phi\mathbf{e_{Fb}} \tag{6}$$

$$\mathbf{e_{Bb}} = \sin\phi\mathbf{e_{Fa}} + \cos\phi\mathbf{e_{Fb}} \tag{7}$$

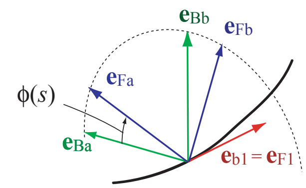

Fig. 5. Definition of $\phi(s)$

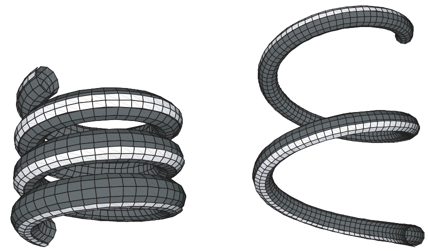

(a) Example (1)

(b) Example (2)

Fig. 6. Spirals of Bellows Model

The following equation is derived by $\frac{d\mathbf{e_{F1}}}{ds} = \frac{d\mathbf{e_{B1}}}{ds}$, (4) and (5).

$$\kappa\mathbf{e_{Fa}} = \kappa_b\mathbf{e_{Ba}} - \kappa_a\mathbf{e_{Bb}} \tag{8}$$

And the following equation is derived by substituting (6) and (7) for (8) to eliminate $\mathbf{e_{Ba}}$ and $\mathbf{e_{Bb}}$.

$$\kappa_F = -\kappa_{Ba}\sin\phi + \kappa_{Bb}\cos\phi \tag{9}$$

$$0 = \kappa_{Ba}\cos\phi + \kappa_{Bb}\sin\phi \tag{10}$$

From (4), (5) and (6), the following equation is obtained.

$$\begin{aligned} \frac{d(\mathbf{e_{Fa}}\cdot\mathbf{e_{Ba}})}{ds} &= \frac{d\mathbf{e_{Fa}}}{ds}\cdot\mathbf{e_{Ba}} + \mathbf{e_{Fa}}\cdot\frac{d\mathbf{e_{Ba}}}{ds} \\ &= -\tau\sin\phi \end{aligned} \tag{11}$$

On the other hand, $\mathbf{e_{Fa}}\cdot\mathbf{e_{Ba}} = \cos\phi$ holds true by (6). Finally, the following equation is obtained.

$$\begin{aligned} \frac{d\cos\phi}{ds} &= -\frac{d\phi}{ds}\sin\phi = -\tau\sin\phi \\ \therefore \frac{d\phi}{ds} &= \tau \end{aligned} \tag{12}$$

And the following are the initial conditions.

$$\left\{\begin{array}{l} \mathbf{c_B} = \mathbf{c_F} \\ \mathbf{e_{B1}} = \mathbf{e_{F1}} \\ \mathbf{e_{Ba}} = \cos\phi\mathbf{e_{Fa}} - \sin\phi\mathbf{e_{Fb}} \\ \mathbf{e_{Bb}} = \sin\phi\mathbf{e_{Fa}} + \cos\phi\mathbf{e_{Fb}} \end{array}\right. \tag{13}$$

The set of (9), (10), (12) and (13) is the necessary condition for making 2 models draw a same backbone curve.

Next, we prove the above set is also the sufficient condition. For this goal, we substitute (9), (10), (12) for (5) and make sure that the backbone curve of (5) becomes equal to that of

(4). As the preparation, we introduce new unit vectors defined by following equations.

$$\mathbf{r_a} = \cos\phi\mathbf{e_{Ba}} + \sin\phi\mathbf{e_{Bb}} \tag{14}$$

$$\mathbf{r_b} = -\sin\phi\mathbf{e_{Ba}} + \cos\phi\mathbf{e_{Bb}} \tag{15}$$

Firstly $\mathbf{e_{Ba}}$ and $\mathbf{e_{Bb}}$ are eliminated from (5) by (14) and (15). Then we obtain following equations by rearranging terms using (9), (10), (12).

$$\left\{\begin{array}{lcl} \dfrac{d\mathbf{c_B}}{ds} & = & \mathbf{e_{B1}} \\ \dfrac{d\mathbf{e_{B1}}}{ds} & = & \kappa_{Fb}(s)\mathbf{r_a} \\ \dfrac{d\mathbf{r_a}}{ds} & = & -\kappa_{Fb}(s)\mathbf{e_{B1}} + \tau_F(s)\mathbf{r_b} \\ \dfrac{d\mathbf{r_b}}{ds} & = & -\tau_F(s)\mathbf{r_a} \end{array}\right. \tag{16}$$

(16) is equal to (4) if we can consider $\mathbf{r_a}$ and $\mathbf{r_b}$ as $\mathbf{e_a}$ and $\mathbf{e_b}$ respectively. So when initial condition (13) is true, $\mathbf{c_B}$ is equal to $\mathbf{c_F}$ in (4). This proved that the set of (9), (10), (12) and (13) is the sufficient condition. After all we proved that the set of (9), (10), (12) and (13) is the necessary and sufficient condition for making the 2 models draw a same backbone curve. (13) is just a initial condition, so the important condition is following 2 equations.

$$\begin{pmatrix} 0 \\ \kappa_{Fb} \end{pmatrix} = \begin{pmatrix} \cos\phi & \sin\phi \\ -\sin\phi & \cos\phi \end{pmatrix} \begin{pmatrix} \kappa_{Ba} \\ \kappa_{Bb} \end{pmatrix} \tag{17}$$

$$\frac{d\phi}{ds} = \tau \tag{18}$$

As you know from (17) and (18), we can obtain κ_{Ba} and κ_{Bb} satisfying the condition as to any τ and κ_{Fb}. This prove that bellows model can draw any spatial curve as the backbone curve. Fig. 6 shows a bellows model drawing a spiral backbone curve. A spiral curve have constant curvature and torsion ($\kappa_F = const., \tau_F = const.$), so κ_{Ba} and κ_{Bb} are calculated from (17) and (18). The lines drawn on models in Fig. 6 means a certain direction of the dorsal reference frames; the line is straight when the backbone curve is straight. Comparing (3) and (6), we know that the lines are similar. This shows the dorsal reference frame expresses the posture of bellows sufficiently and bellows model (5) represents the characteristic of bellows. Fig. 7 shows the comparison of a spiral of a snake and that of a bellows model. The direction of the dorsal reference frame and that of the snake's body are alike, which confirm that snakes has the same characteristics as bellows.

We note that a bellows model can imitate any backbone curve of a Frenet-Serret model, but the opposite is not true. This is explained by the following equation derived from (17).

$$\phi = \tan^{-1}\frac{-\kappa_{Ba}}{\kappa_{Bb}} \tag{19}$$

$$\therefore \tau = \frac{d\phi}{ds} = \frac{\kappa'_{Bb}\kappa_{Ba} - \kappa'_{Ba}\kappa_{Bb}}{\kappa_{Ba}^2 + \kappa_{Bb}^2} \tag{20}$$

This equation shows that if κ_{Ba}/κ_{Bb} is not constant around a point where $\kappa_{Ba} = \kappa_{Bb} = 0$ holds true, τ becomes infinite.

Fig. 7. Spirals of Snake and Bellows Model

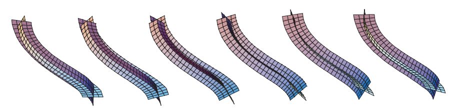

Fig. 8. Lateral Rolling of a Continuous Model

That is the reason why a Frenet-Serret model can not copy all backbone curves of a bellows model. Generally speaking, snake-like robots often have such points where the curvature becomes zero, so Frenet-Serret model is not suitable as a model of a snake-like robot. As we know from Fig. 7, bellows model is adequate as a model of snake-like robots.

We show another important characteristics of bellows model from (18). Because (18) is a first-order differential equation, ϕ has one constant of integration for given τ. ϕ is a function of s defined by Fig. 5, so when the constant of integration varies the dorsal reference frame of bellows model rotates as to that of Frenet-Serret model at the same angle along the whole backbone curve. This means that bellows model has one degree of freedom to rotate the direction of dorsal reference frame around the backbone curve, as it maintains the backbone curve. Fig. 8 shows this motion. This characteristic can be easily confirmed by a flexible straw which has bellows. When we rotate the one end of a bended flexible straw, the other end is also rotated simultaneously regardless of the shape of the straw. (18) is a mathematical explanation of this phenomena. In prior research on snake-like robots, this motion, called "lateral rolling", have been paid attention and explained or realized using discrete mechanism [7][8][9]. (18) gives another explanation using continuous ACM model.

C. Complete Model

We define *complete model* as a model which has no limitation about shape functions, so complete model can realize all shapes possible for ACM. That is why complete model have advantages compared with above 3 models. For example, a snake-like robot equipped with wheels should ground them. If and only if the snake-like robot is a complete model, it can adjust the direction of wheels maintaining the backbone curve.

Here we discuss a condition on that a complete model draws different dorsal reference curves though the backbone curves

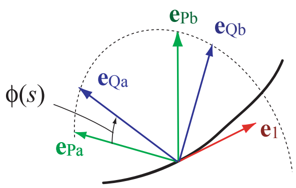

Fig. 9. Definition of $\phi(s)$

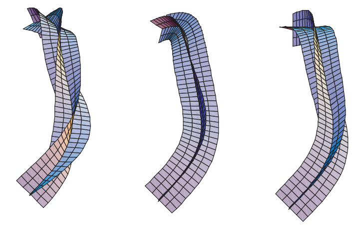

Fig. 10. Different Dorsal Reference Curves with the same backbone curve

are the same. Now we think about 2 dorsal reference curves P, Q, which have the same backbone curve. The relative angle ϕ between these dorsal reference frames is defined as Fig. 9 and now ϕ is known. Firstly, following 6 equations must be true at any s.

$$\frac{d\mathbf{e_1}}{ds} = \kappa_{Pb}(s)\mathbf{e_{Pa}} - \kappa_{Pa}(s)\mathbf{e_{Pb}} \quad (21)$$

$$\frac{d\mathbf{e_{Pa}}}{ds} = -\kappa_{Pb}(s)\mathbf{e_1} + \tau_P(s)\mathbf{e_{Pb}} \quad (22)$$

$$\frac{d\mathbf{e_{Pb}}}{ds} = \kappa_{Pa}(s)\mathbf{e_1} - \tau_P(s)\mathbf{e_{Pa}} \quad (23)$$

$$\frac{d\mathbf{e_1}}{ds} = \kappa_{Qb}(s)\mathbf{e_{Qa}} - \kappa_{Qa}(s)\mathbf{e_{Qb}} \quad (24)$$

$$\frac{d\mathbf{e_{Qa}}}{ds} = -\kappa_{Qb}(s)\mathbf{e_1} + \tau_Q(s)\mathbf{e_{Qb}} \quad (25)$$

$$\frac{d\mathbf{e_{Qb}}}{ds} = \kappa_{Qa}(s)\mathbf{e_1} - \tau_Q(s)\mathbf{e_{Qa}} \quad (26)$$

In addition, the following equations are also true from Fig. 9.

$$\mathbf{e_{Pa}} = \cos\phi\mathbf{e_{Qa}} - \sin\phi\mathbf{e_{Qb}} \quad (27)$$

$$\mathbf{e_{Pb}} = \sin\phi\mathbf{e_{Qa}} + \cos\phi\mathbf{e_{Qb}} \quad (28)$$

From above 8 equations we can derive the necessary condition. Firstly, the following equations are obtained from (21), (24) and (27).

$$\begin{pmatrix} \kappa_{Qa} \\ \kappa_{Qb} \end{pmatrix} = \begin{pmatrix} \cos\phi & \sin\phi \\ -\sin\phi & \cos\phi \end{pmatrix} \begin{pmatrix} \kappa_{Pa} \\ \kappa_{Pb} \end{pmatrix} \quad (29)$$

Secondly, the following equation is derived from (22), (25), (27) and (28).

$$\begin{aligned} \frac{d(\mathbf{e_{Qa}} \cdot \mathbf{e_{Pa}})}{ds} &= \frac{d\mathbf{e_{Qa}}}{ds} \cdot \mathbf{e_{Pa}} + \mathbf{e_{Qa}} \cdot \frac{d\mathbf{e_{Pa}}}{ds} \\ &= (-\tau_Q + \tau_P)\sin\phi \quad (30) \end{aligned}$$

On the other hand, $\mathbf{e_a} \cdot \mathbf{e_2} = \cos\phi$ is true from (27). So the following equation holds true.

$$\begin{aligned} \frac{d\cos\phi}{ds} = -\frac{d\phi}{ds}\sin\phi &= (-\tau_Q + \tau_P)\sin\phi \\ \therefore \tau_Q &= \frac{d\phi}{ds} + \tau_P \quad (31) \end{aligned}$$

(29) and (31) are the necessary condition when a complete model draw different dorsal reference curves with the same backbone curve, and we can show they are also the sufficient condition by the exactly same way in section IV-B. So complete model can vary the direction of its dorsal reference frame keeping the backbone curve if it follows (29) and (31) as shown in Fig. 10. The backbone curves in Fig. 10 are exactly same, though the dorsal reference curves are different.

We note that if $\kappa_{Qa} = 0$ and $\tau_P(s) = 0$ are substituted in (29) and (31), the equations are equal to (17) and (18) in section 4.2. This is understandable because $\kappa_{Pa} = 0$ and $\tau_Q(s) = 0$ indicates that the dorsal reference curves P, Q are the shape of Frenet-Serret model and bellows model respectively. This shows that (29) and (31) are generalization of (17) and (18).

V. Conclusion and Future Work

In this paper, we proposed a method dealing with ACM's 3-dimensional shape. In addition, based on this method we classified ACM into important 4 models and discuss each characteristics. Especially we dealt with bellows model in detail, which is important for snake-like robots, and proved mathematically that it can draw any spatial curve and it can rotate the body around the backbone curve.

Now we study about application of a continuous ACM model in control of real mechanisms, for example how to fit a discrete mechanism into a continuous model. In addition, we construct several ACM as shown in Fig. 1 and conduct experiments with them. We plan to study both of control and mechanism of ACM using them.

References

[1] S. Hirose, *Biologically Inspired Robots*, Oxford University Press, 1993.

[2] Gregory S. Chirikjian, Joel W. Burdick, *A Modal Approach to Hyper-Redundant Manipulator Kinematics* IEEE Transaction on Robotics and Automation, vol. 10, No. 3, pp343-354, 1994.

[3] H. Mochiyama, T. Suzuki, *Kinematics and Dynamics of a Cable-like Hyper-flexible Manipulator* Proc. of the 2003 IEEE Int. Conf. on Robotics and Automations, pp. 3672-3677, 2003.

[4] H. Date, M. Sanpei, S. Nakaura, *Motion Control of 3D Snake Robot on a Surface*, SICE 2nd Conference of Control Division, pp17-20, 2002. (In Japanese)

[5] Bryan A. Jones, Ian D. Walker, *A New Approach to Jacobian Formulation for a Class of Multi-Section Continuum Robots*, Proc. of 2005 IEEE Int. Conf. on Robotics and Automation, pp. 3279-3284, 2005.

[6] M. Masuda, *Snakes and Lizards*, Akane Shobo, 1988. (In Japanese)

[7] K. Dowling, *Limbless Locomotion: Learning to Crawl*, Proc. of 1999 IEEE Int. Conf. on Robotics and Automation, pp. 3001-3006, 1999.

[8] T. Kamegawa, F, Matsuno, R. Chatterjee, *Proposition of Twisting Mode of Locomotion and GA Based Motion Planning for Transition of Locomotion Mode of 3-Dimensional Snake-like robot*, Proc. of the 2002 IEEE Int. Conf. on Robotics and Automations, pp. 1507-1512, 2002.

[9] L. Chen, Y. Wang, S. Ma, B. Li, *Studies on Lateral Rolling Locomotion fo a Snake Robot*, Proc. of the 2004 IEEE Int. Conf. on Robotics and Automation, pp. 5070-5074, 2004.